

Three-Pole Tunable Filters with High Rejection using Mixed $\lambda/4$ Resonators and Asymmetric $\lambda/2$ Resonators

Zhiyuan ZHAO^{1,2}, Jiang CHEN², Lin YANG², Kunhe CHEN²

¹ Institute of Communications Engineering, PLA University of Science and Technology, Nanjing 210007, China

² Nanjing Telecommunication Technology Institute, Nanjing 210007, China

zhaozhiyuan1986@sina.com, chenjiang999@sina.com

Abstract. A novel three-pole tunable bandpass filter using varactor-loaded quarter-wavelength combline and asymmetric half-wavelength resonators is proposed in this paper. A nearly constant 3-dB absolute bandwidth is 150 ± 13 MHz (10.7%–6.9% fractional bandwidth) within the tuning range of 1.4–2.0 GHz (42.8%). The filter is designed on a Rogers substrate with $\epsilon_r = 2.2$ and $h = 1$ mm with its insertion loss varying from 3.6 dB to 2.8 dB and return loss better than 10 dB over the entire tuning range. The creation of two transmission zeros near the passband edges is analyzed by the even-odd-method. By using dissimilar resonators, the proposed tunable filter could obtain > 33 dB rejection levels at the second harmonics. The measured results show good agreement with the simulated ones.

Keywords

Three-pole tunable filters, combline resonators, modified combline resonators, constant absolute bandwidth (CABW), transmission zeros (TZs), varactor-tuned.

1. Introduction

Electronically tunable or reconfigurable pre-select microwave filters significantly improve the overall performance of multi-bands and multi-functions wireless communication systems, which bring the reduction of the system size, complexity and cost. Planar tunable bandpass filters (BPFs) can be realized by varactor diodes [1], ferroelectric diodes [2], or RF micro-electro-mechanical systems (RF-MEMS) devices [3]. However, the varactor-diode filters are widely studied due to the advantages of continuous and high-speed tuning and economical fabrication.

Due to compactness and ease of integration, combline and modified combline resonators loaded by varactor diodes, commonly used in small-size tunable filters for the RF front end, have been studied in numerous literatures [4]–[11]. However, the combination of quarter-wavelength ($\lambda/4$) combline and asymmetric half-length ($\lambda/2$) resonators, especially for realizing a constant absolute bandwidth

(CABW) of three-pole tunable filter with high rejection, has not been reported. Hunter and Rhodes firstly described that the optimum electrical length is approximately 53° at the center frequency of the tuning range for achieving the constant bandwidth of the stripline tunable filter [4]. For microstrip-line tunable filter, a systematic approach was presented to choose the tunable filter design parameters [5]. In [6], a tunable combline filter with plural transmission zeros originating from source-load and multi-resonators coupling was realized. Note that most microstrip combline or modified combline filters only have transmission zeros in the lower stopband or upper stopband, and this leads to an asymmetrical transmission response and poor rejection in the stopband without transmission zeros. Yi-Chyun Chiou et. al. proposed a non-adjacent resonator coupling to generate an extra zero at the lower band, except the intrinsic zero at the upper stopband [7]. In [8], there were two transmission zeros at both sides of the passband, respectively, however the source-load coupling structure was complicated. In [9], there were two transmission zeros near the passband due to the tap connections of input and output port, however the rejection level in the stopband was not high enough without adding the bandpass network to the two ends. Therefore, it remains difficult to realize a high-rejection tunable filter with CABW and two transmission zeros within a wide tuning range.

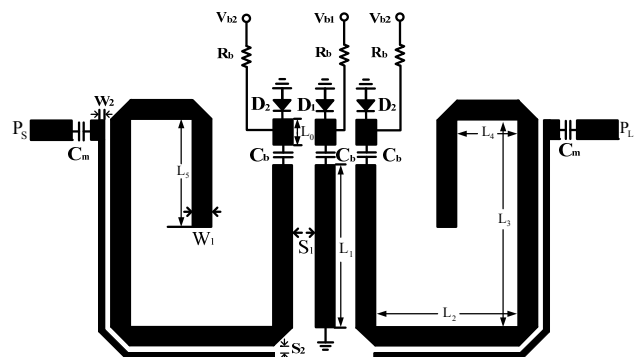


Fig. 1. Proposed three-pole tunable BPF using mixed $\lambda/4$ combline and asymmetric $\lambda/2$ resonators.

This paper proposes a new three-pole tunable filter with two transmission zeros using mixed $\lambda/4$ combline and asymmetric $\lambda/2$ resonators, as shown in Fig. 1. The design

aim is to maintain the absolute bandwidth constant and obtain high rejection. It consists of an asynchronously varactor-tuned $\lambda/4$ combline resonator between the two varactor-loaded asymmetric $\lambda/2$ resonators. Parallel-coupled-lines are selected as the external coupling structure to achieve impedance matching across a wide tuning range without any other tuning components [10]. By properly controlling the bias voltages, a high-rejection tunable filter with nearly constant absolute bandwidth within a wide frequency tuning range can be realized.

This paper is organized as follows. The characteristic of the proposed filter topology is introduced and design theory is analyzed in Section 2. In Section 3, experimental results of a built prototype are shown. Finally, the conclusions of this work are drawn in Section 4.

2. Tunable Filter Theory

2.1 Bandwidth Characteristic of the Coupled Resonators

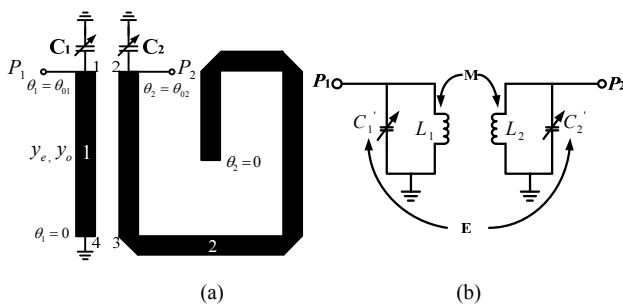


Fig. 2. (a) Coupled varactor-loaded combline and modified-combline resonators, and (b) its equivalent circuit.

The design is based on varactor-loaded $\lambda/4$ combline resonator and varactor-loaded asymmetric $\lambda/2$ modified-combline resonators [9]. Fig. 2 presents a coupled-resonator section of the proposed tunable filter and its simplified equivalent circuit. The lumped-element capacitances are $C_1' = C_c' + C_1$ and $C_2' = C_a' // C_2$, and the inductances are L_1 and L_2 , where L_1 and C_c' are the equivalent inductor and capacitor of the $\lambda/4$ combline resonator, respectively, L_2 and C_a' are the equivalent inductor and capacitor of the asymmetric $\lambda/2$ modified-combline resonator, respectively [11]. The coupling coefficient of the equivalent coupled resonators model in Fig. 2 is calculated by energetic coupling approach [12]. Assuming weak coupling condition ($k_M k_E \ll 1$), the coupling coefficient is determined as

$$k \approx k_M + k_E = \frac{(k_L' - k_C')[\cos \Delta\theta - \cos(\theta_{02} + \theta_{01})]}{\sqrt{(2\theta_{01} + \sin 2\theta_{01})(2\theta_{02} - \sin 2\theta_{02})}} + \frac{2(k_L' + k_C')\theta_{01} \sin \Delta\theta}{\sqrt{(2\theta_{01} + \sin 2\theta_{01})(2\theta_{02} - \sin 2\theta_{02})}} \quad (1)$$

$$\Delta\theta = \theta_{02} - \theta_{01} \quad (2)$$

where, k_L' and k_C' are the inductive and capacitive coupling coefficients per unit length in the coupling region. θ_{01} ($\theta_{01} < \pi/4$) and θ_{02} ($\theta_{02} > \pi/2$) indicate electrical lengths of the $\lambda/4$ combline resonator and the asymmetric $\lambda/2$ resonator, respectively. Using the standard differentiation procedure, given $\theta_{02} = 4\theta_{01}$, it can be calculated that the optimum electrical length of θ_{01} in the midband of the tuning range. The crude optimum electrical length of the $\lambda/4$ combline resonator corresponds to the frequency at which the bandwidth is maximized.

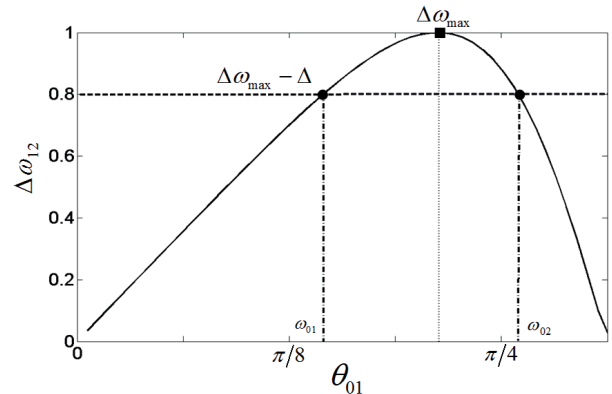


Fig. 3. Normalized bandwidth of the proposed architecture using quasi-TEM resonators.

Fig. 3 is a plot of normalized coupling bandwidth $\Delta\omega_{12}$ ($\Delta\omega_{12} = k\omega_0$) versus θ_{01} according to (1) when quasi-TEM resonators are used, with $\omega_0 = \theta_{01}$. If the allowed percentage change of bandwidth is $\pm 10\%$, a wide center frequency tuning range (ω_{01}, ω_{02}) can be obtained to fulfill the bandwidth requirement $[\Delta\omega_{\max} - \Delta, \Delta\omega_{\max}]$. Due to the linear relationship between electrical length and frequency, the plot shows the bandwidth dependence on the tuning frequency. The electrical length corresponding to $\Delta\omega_{\max}$ is the optimum resonator length ($\theta_{01} = 39^\circ$) at the midband.

2.2 Analysis of the Coupled Resonators

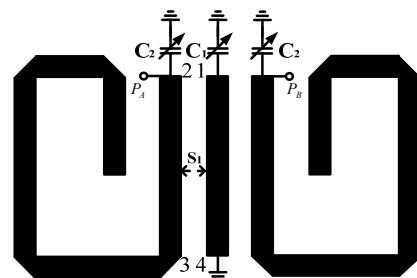


Fig. 4. The three coupled-resonators without I/O coupling structure.

In the analysis of the three coupled-resonators of the proposed tunable filter, the Y-parameter is adopted. Fig. 4 is three coupled-resonators without I/O coupling structure. The reference ports (P_A and P_B) are added for deriving the admittance matrix, the Y-parameter matrix of the two asynchronously coupled-resonators is calculated as

$$Y = \begin{bmatrix} y_{11} - \frac{y_{13}y_{31}}{y_{33} + jY_0 \tan \Delta\theta} & y_{12} - \frac{y_{13}y_{32}}{y_{33} + jY_0 \tan \Delta\theta} \\ y_{21} - \frac{y_{13}y_{32}}{y_{33} + jY_0 \tan \Delta\theta} & y_{22} - \frac{y_{23}y_{32}}{y_{33} + jY_0 \tan \Delta\theta} \end{bmatrix} \quad (3)$$

And the four-port Y parameters of the parallel coupled-line are [13],

$$y_{11} = y_{22} = y_{33} = -\frac{j}{2}(Y_{ro} + Y_{re}) \cot \theta_{01}, \quad (4a)$$

$$y_{12} = y_{21} = -\frac{j}{2}(Y_{ro} - Y_{re}) \cot \theta_{01}, \quad (4b)$$

$$y_{13} = y_{31} = -\frac{j}{2}(Y_{ro} - Y_{re}) \csc \theta_{01}, \quad (4c)$$

$$y_{23} = y_{32} = -\frac{j}{2}(Y_{ro} + Y_{re}) \csc \theta_{01} \quad (4d)$$

where Y_{re} , Y_{ro} are the even- and odd-mode characteristic admittances of the parallel coupled-line, respectively.

The resonant angular frequency ω_0 can be found by the following equation, ($i = 1, 2$).

$$\text{Im}[Y_{ii}(\omega_0)] + \omega_0 C_i = 0 \quad (5)$$

For the filter composed of two varactor-loaded asymmetric $\lambda/2$ resonators, their fundamental resonant frequency is f_0 , and the second-order spurious response is at the frequency higher than $2f_0$. Furthermore, that composed of a varactor-loaded $\lambda/2$ combline resonator has spurious passband far from $3f_0$. Therefore, the rejection level of the second harmonics of the proposed filter in Fig. 1 can be improved significantly.

The coupling coefficient of the coupled resonators is [11]

$$k_{12} = \frac{\text{Im}[Y_{12}(\omega_0)]}{\sqrt{b_1 b_2}} = \frac{BW}{f_0 \sqrt{g_1 g_2}} \quad (6)$$

where BW is the 3-dB absolute bandwidth, g_1 , g_2 are the element values of low-pass prototype filter, respectively. And the slope parameter b_1 and b_2 are derived as [13]

$$b_i = \frac{\omega_0}{2} \frac{\partial \text{Im}[Y_{ii}]}{\partial \omega} \Big|_{\omega=\omega_0} + \frac{\omega_0 C_i}{2}. \quad (7)$$

2.3 Transmission Zeros Creation

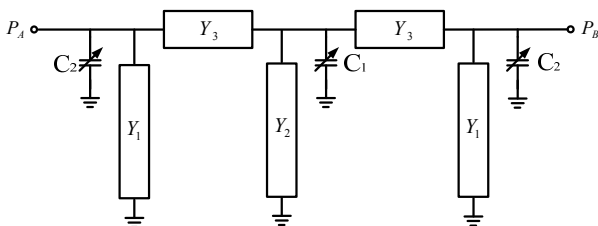


Fig. 5. Equivalent circuit model of the three coupled-resonators.

As was explained in the past literatures, adding I/O coupling structure shifts the transmission zero at infinite frequency downwards, but it does not really add a zero. For facilitating the analysis of the TZs' location, the I/O matching networks are not calculated. Since the topology is symmetrical to the center plane, the S -parameter of the three coupled resonators can be calculated by using the even-odd-mode method [13]. It is assumed that the even- and odd-mode electrical lengths of the parallel symmetrical pair of coupled-lines are identical to the value of θ_{01} , and the parasitic effects of the grounded via-holes and the line discontinuity due to the DC block capacitor C_b are ignored. Fig. 5 presents the exact equivalent circuit model of the three coupled-resonators in Fig. 4. In this circuit, $Y_1 = Y_{22} - Y_3$, $Y_2 = Y_{11} - Y_3$, $Y_3 = -Y_{12}$, where Y_{ij} is the element of the Y matrix in (3).

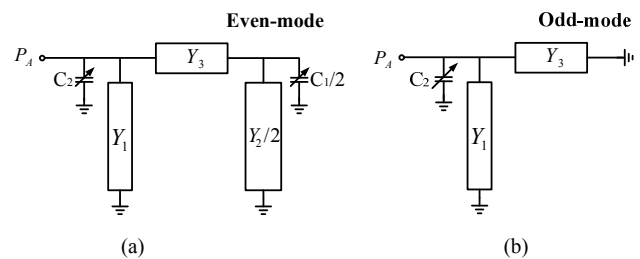


Fig. 6. (a) Its equivalent even-mode circuit, and (b) its equivalent odd-mode circuit in Fig. 5.

Fig. 6 is the equivalent even- and odd-mode circuit obtained by placing a short or open circuit at the symmetric plane. The even- and odd-mode input admittance Y_{Ae} and Y_{Ao} seen from port P_A can be respectively solved by (8) and (9)

$$Y_{Ae} = j\omega C_2 + Y_1 + \frac{Y_3(Y_2 + j\omega C_1)}{Y_2 + 2Y_3 + j\omega C_1}, \quad (8)$$

$$Y_{Ao} = j\omega C_2 + Y_1 + Y_3. \quad (9)$$

By superposition, the transfer function S_{21} can then be written as [13]

$$S_{21} = \frac{Y_0(Y_{Ae} - Y_{Ao})}{(Y_0 + Y_{Ae})(Y_0 + Y_{Ao})} \quad (10)$$

where Y_0 is terminal admittance. Enforcing $S_{21} = 0$ or $Y_{Ae} - Y_{Ao} = 0$, the two transmission zero frequencies can be solved. As can be seen in the above transcendental equations, it is not easy to obtain the explicit solution of the TZs' location.

The transmission response is obtained by feeding the three coupled resonators at P_A and P_B , and the S_{21} response indicates that the filter possesses three poles (f_{p1} through f_{p3}) and two transmission zeros (f_{z1} and f_{z2}), as shown in Fig. 7. One transmission zero appears at the lower stopband, and the other appears at the upper stopband. The TZs creation is usually due to the multiple coupling paths, which means several signals cancel each others at a certain frequency. According to (8)-(10), the transmission zero is a function of the loading capacitance, so they move with the center

frequency of the filter varied by controlling the biasing voltages.

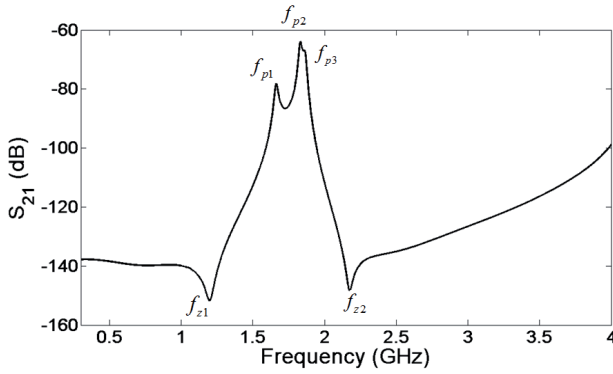


Fig. 7. S_{21} response of Fig. 4 with weakly capacitive coupling at its two ports.

2.4 Extraction of k_{12} and Q_e of the Tunable Filter

As the center frequency of the filter is varied, all of the filter parameters change. Thus, the coupling coefficients between resonators are always changed. To assure CABW, the desired coupling coefficient must satisfy the conditions described in [3]. The gap S_1 is chosen so that the two asynchronously tuned resonators are coupled through a suitable coupling coefficient k_{12} . The coupling coefficient k_{12} of the coupled resonators can be calculated by [13]

$$k_{12} = \pm \frac{1}{2} \left(\frac{f_{02}}{f_{01}} + \frac{f_{01}}{f_{02}} \right) \sqrt{\frac{(f_{p2}^2 - f_{p1}^2)^2}{f_{p2}^2 + f_{p1}^2} - \frac{(f_{02}^2 - f_{01}^2)^2}{f_{02}^2 + f_{01}^2}} \quad (11)$$

where f_{01} , f_{02} are resonant frequencies of each single resonator, f_{p1} and f_{p2} are frequencies of the two peaks. The choice of the sign in (4) depends on the definition of electric and magnetic coupling.

To maintain nearly constant absolute bandwidth, the external quality factor Q_e should increase as the frequency shifts upward. This can be realized by using the parallel-line structure as shown in Fig. 1. The geometrical dimensions and capacitance of the matching capacitor C_m of the I/O structure can be determined by matching the singly loaded Q. The required Q_e for a 3-pole filter is given by [13]

$$Q_e = \frac{f_0}{\Delta f_{\pm 90^\circ}} = \frac{g_0 g_1 f_0}{BW} \quad (12)$$

where $\Delta f_{\pm 90^\circ}$ is determined from the frequency at which the phase shifts $\pm 90^\circ$ with respect to the absolute phase at f_0 .

3. Design and Experimental Verification of Tunable Filter

A nearly CABW three-pole tunable filter with high rejection using $\lambda/4$ combline and asymmetric $\lambda/2$ resonators

is presented in this section to verify the analysis above. A full-wave electromagnetic simulator, Computer Simulation Technology (CST2009) Microwave Studio and Design Studio software packages are employed for the circuit dimensions of final filter simulation. The designed filter is simulated and fabricated in microstrip technology with the following specifications:

Frequency tuning range: 1.4-2.0 GHz;

Passband bandwidth: 150 ± 10 MHz;

Number of poles: three;

Type: 0.04-dB ripple Chebyshev at 1.7 GHz.

3.1 Design Procedure

Step 1). Subjecting to the specifications, select the three-pole low-pass prototype with elements g_i , $i=0, \dots, 4$. Then calculate the external quality factors and coupling coefficient according to (6) and (12).

Step 2). Determine the dimensions of the proposed tunable resonators. The electrical length of the combline resonator is set to be 39° ($\theta_{01} = 39^\circ$, $\theta_{02} = 4\theta_{01} = 156^\circ$) at 1.7 GHz. The characteristic impedance of combline filter is traditionally 71 or 72 Ω to obtain the optimum unloaded Q [11]. For minimizing the size of the circuit, especially the asymmetric half-wavelength resonator, we choose a little higher characteristic impedance ($W_1 = 1$ mm). The gap S_1 between $\lambda/4$ combline resonator and asymmetric $\lambda/2$ resonators can then be determined to satisfy k_{12} . The parameters of the I/O structure are typically chosen to be a high impedance line for tight coupling. The matching capacitor C_m , the gap S_2 , and the width W_2 of the line are then chosen to satisfy Q_e .

Step 3). Finally, the optimization of circuit dimensions of filter is employed CST2009 EM simulator. The electrical length of the comb-line resonator is optimized to be 8 mm (27°) at 1.7 GHz because of the additional equivalent electrical lengths of grounding via-holes, grounding pads and components of DC blocking capacitor and varactor.

According to the extraction method of coupling coefficient and external quality factor in [13], the k_{12} and Q_e versus different center frequencies of the tunable filter is extracted and plotted in Fig. 8 with the desired values for the constant absolute bandwidth. Due to the inconsistency between the simulated k_{12} , Q_e and the desired ones, the ripple of the filter will change and the absolute bandwidth will vary as the frequency shifts downward or upward from the mid-band.

For the optimized resonators, the capacitance of the loading varactors C_1 and C_2 corresponding to the resonant frequency is plotted in Fig. 9 for comparison. The simulated results agree well with the calculated ones by (5).

The filter is designed on Rogers RT5880 substrate ($\epsilon_r = 2.2$, $h = 1$ mm, and $\tan \delta = 0.0009$) with overall size of $\sim 40 \times 36$ mm², as shown in Fig. 10.

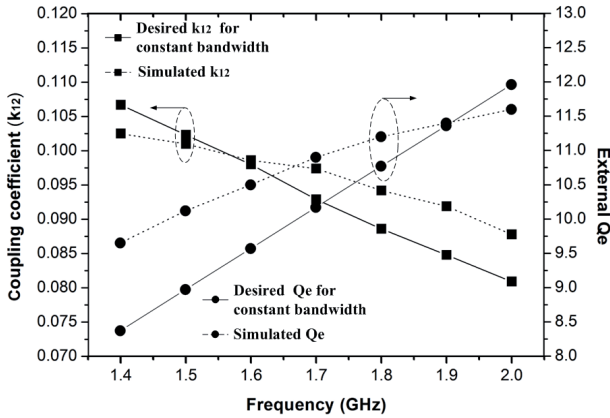


Fig. 8. Desired and simulated coupling coefficients and Q_e of the proposed filter.

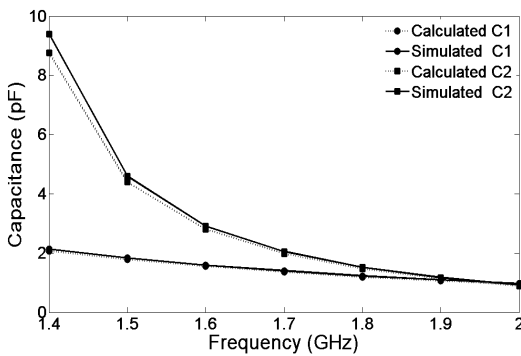


Fig. 9. Calculated and simulated capacitance of the loading varactors for the optimized resonators.

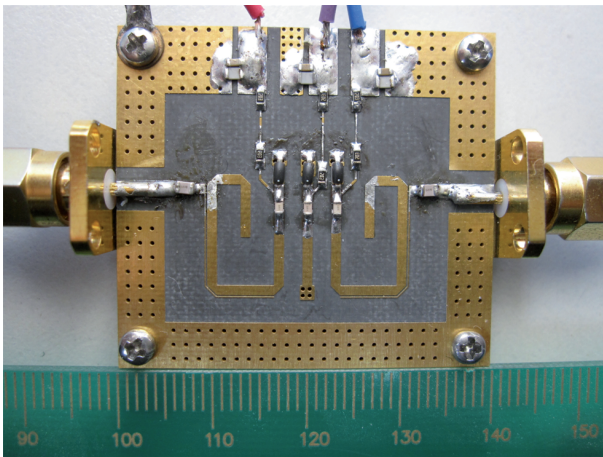


Fig. 10. Photograph of the fabricated 3-pole tunable filter including biasing circuits.

W_1 / W_2	$L_0 / L_1 / L_2 / L_3 / L_4 / L_5$	S_1 / S_2	C_m (pF) / C_b (pF)
1 / 0.1	2 / 8 / 6 / 10.6 / 2.5 / 5.5	2 / 0.1	5.6 / 15

Tab. 1. Dimensions for the filter (Dimensions are in millimeters).

The physical dimensions of the filter are summarized in Tab. 1. The matching capacitor C_m and DC blocking capacitor C_b are realized by ATC 600S series capacitors. The DC blocking capacitor has a high self-resonant

frequency of over 2.5 GHz, which works as open circuit at DC frequency and short circuit at RF frequency. The capacitors C_1 and C_2 are implemented by MA46H202-1088 GaAs diodes. MA46H202 varactor diodes (C_1 or $C_2 = 0.6-11$ pF, $R_s = 0.2-0.9 \Omega$, over a 22 V reverse bias range) are selected as D_1 and D_2 for frequency tuning, respectively. The biasing circuits are realized using two 100-k Ω resistors to minimize RF signal leakage.

3.2 Measurements

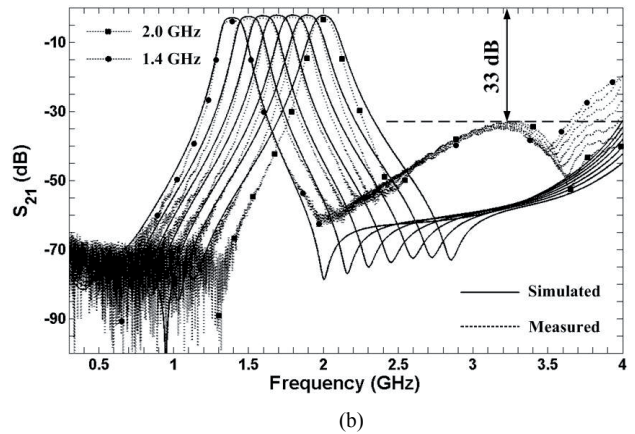
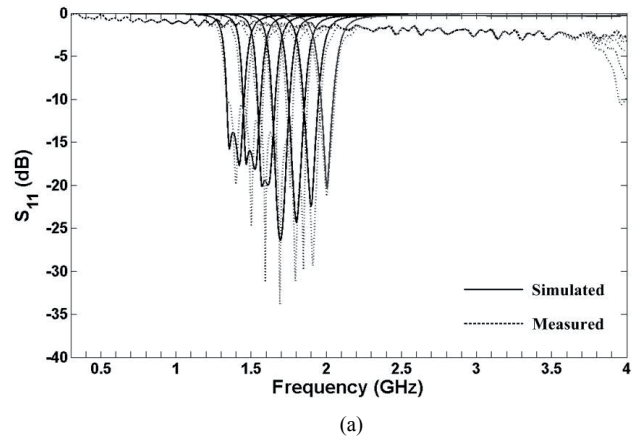


Fig. 11. Measured and simulated S -parameters of the proposed tunable BPF. (a) S_{11} . (b) S_{21} .

The measured frequency responses of the designed filter with the center frequency tuning obtained by using Agilent N5230A network analyzer are in good agreement with the simulation results, as shown in Fig. 11. The measured return loss ($|S_{11}|$) is worse than the simulation results due to the inconsistency of the varactor diodes biased by only one bias voltage for the asymmetric $\lambda/2$ resonators, however better than 10 dB for all states. The 3-dB absolute bandwidth is maintained nearly constant about 150 MHz (150 ± 13 MHz) over the entire center frequency tuning range from 1.4 GHz to 2.0 GHz (a wide tuning range of 42.8%). The bandwidth slightly increases at the midband frequency and decreases at the both ends of the tuning range. The characteristic of bandwidth variation is consistent with that of Fig. 3. Because of the effect of the

package inductances of the varactor diodes and parasitic inductance coupling among the via-holes, the passband bandwidth has slight variation between simulation and measurement. Its insertion loss ($|S_{21}|$) varies from 3.6 dB to 2.8 dB due to the low overall unloaded Q of the resonators by using varactors [14]. The insertion loss improves as the center frequency is tuned to the higher end of the tuning range, and it is related to the characteristic of the varactor diodes under different bias condition and the variation of fractional BW (10.7% at lower end and 6.9% at higher end). The discrepancies mainly result from fabrication tolerance in the implementation and the simulation error between SPICE models and actual varactor diodes.

Note that the two transmission zeros near to passband are shifted with the center frequency varied, and the rejection of the lower and upper stopbands remains high with the tuning. Furthermore, the extra zero appears at the higher side due to the package inductance of the varactor diodes, which can enhance the rejection of the second harmonics (> 33 dB). By using dissimilar resonators [15], the rejection level is > 20 dB in the stopband from $1.07f_0$ to $2.85f_0$. The nonlinear distortion performance is another important figure of merit due to the involvement of the varactor. The measured 1-dB compression point at the filter input is higher than 8 dBm over the tuning frequency. The measured IIP3 is ranging from 33 dBm to 38 dBm for $\Delta f = 1$ MHz, meeting most of the requirements for software-defined radio applications. The summary of the measured results is shown in Tab. 2.

f_0 (GHz)	I.L. (dB)	BW (MHz)	PI (dBm)	IIP3 (dBm)	V_{b1} (V)	V_{b2} (V)
1.4	3.6	150	8	33	5.45	0.5
1.7	3.0	163	9	38	8.65	6.0
2.0	2.8	137	8.5	36	13.2	14.9

Tab. 2. Measured results of the tunable filter.

4. Conclusions

In this paper, we proposed a novel three-pole tunable filter topology with high rejection by using mixed varactor-loaded $\lambda/4$ combline and asymmetric $\lambda/2$ resonators. A 1.4-2.0 GHz three-pole microstrip-line tunable filter with a nearly constant 3-dB absolute bandwidth of 150 ± 13 MHz and the rejection level > 33 dB at the second harmonics is simulated, fabricated, and measured. The measured results agree well with the simulated ones.

Acknowledgements

This work was supported by Key Pre-research Foundation of PLA university of Science and Technology under grant KY63ZLXY1301. The authors would like to thank M/A-COM Corporation for the high-performance varactor diodes and Rogers Corporation for the low-loss substrate.

References

- [1] WONG, P. W., HUNTER, I. C. Electronically tunable filters. *IEEE Microwave Magazine*, 2009, vol. 10, no. 6, p. 46–54.
- [2] HONG, J. S. Reconfigurable planar filters. *IEEE Microwave Magazine*, 2009, vol. 10, no. 6, p. 73–83.
- [3] REBEIZ, G. M., REINES, I. C., EL-TANANI, M. A., ET AL. Tuning in to RF MEMS. *IEEE Microwave Magazine*, 2009, vol. 10, no. 6, p. 55–72.
- [4] HUNTER, I. C., RHODES, J. D. Electronically tunable microwave bandpass filters. *IEEE Transactions on Microwave Theory and Techniques*, 1982, vol. 30, no. 9, p. 1354–1360.
- [5] TORREGROSA-PENALVA, G., LOPEZ-RISUENO, G., ALONSO, J. I. A simple method to design wide-band electronically tunable combline filters. *IEEE Transactions on Microwave Theory and Techniques*, 2002, vol. 50, no. 1, p. 172–177.
- [6] SANCHEZ-RENEADO, M. High-selectivity tunable planar combline filter with source/load-multiresonator Coupling. *IEEE Microwave Wireless Components Letter*, 2007, vol. 17, no. 7.
- [7] CHIOU, Y. C., REBEIZ, G. M. A quasi elliptic function 1.75-2.25 GHz 3-pole bandpass filter with bandwidth control. *IEEE Transactions on Microwave Theory and Techniques*, 2012, vol. 60, no. 2, p. 244–249.
- [8] EL-TANANI, M. A., REBEIZ, G. M. A two-pole two-zero tunable filter with improved linearity. *IEEE Transactions on Microwave Theory and Techniques*, 2009, vol. 57, no. 4, p. 830–839.
- [9] ZHANG, X. Y., XUE, Q., CHAN, C. H., ET AL. Low-loss frequency-agile bandpass filters with controllable bandwidth and suppressed second harmonic. *IEEE Transactions on Microwave Theory and Techniques*, 2010, vol. 58, no. 6, p. 1557–1564.
- [10] PARK, S. J., REBEIZ, G. M. Low-loss two-pole tunable filters with three different predefined bandwidth characteristics. *IEEE Transactions on Microwave Theory and Techniques*, 2008, vol. 56, no. 5, p. 1137–1148.
- [11] MATTHAEI, G. L., YOUNG, L., JONES, E. M. T. *Microwave Filters Impedance-Matching Networks, and Coupling Structures*. Norwood, MA: Artech House, 1980.
- [12] GUYETTE, A. C. Alternative architectures for narrowband varactor-tuned bandpass filters. In *Proceedings of the 39th European Microwave Conference*. Rome (Italy), 2009, p. 1828–1831.
- [13] HONG, J. S., LANCASTER, M. J. *Microstrip Filters for RF/Microwave Applications*. New York: Wiley, 2001.
- [14] BROWN, A. R., REBEIZ, G. M. A varactor tuned RF filter. *IEEE Transactions on Microwave Theory and Techniques*, 2000, vol. 48, no. 7, p. 1157–1160.
- [15] LI, Y. C., ZHANG, X. Y., XUE, Q. Bandpass filter using discriminating coupling for extended out-of-band suppression. *IEEE Microwave Wireless Components Letter*, 2010, vol. 20, no. 7, p. 369–371.

About Authors ...

Zhiyuan ZHAO was born in 1986. He received his bachelor's degree from Lanzhou University in 2008, and received his master's degree from PLA University of Science and Technology in 2011. He is now a Ph. D candidate in the Institute of Communications Engineering, PLA University of Science and Technology, Nanjing, China. His research interests include microwave and RF tunable filters.

Jiang CHEN was born in 1965 and he is now a professor in Nanjing Telecommunication Technology Institute, Nanjing, China. His research interests include RF power amplifiers and RF filters.

Lin YANG was born in 1974 and he is now an engineer in

Nanjing Telecommunication Technology Institute, Nanjing, China. His research interests include RF power amplifiers.

Kunhe CHEN was born in 1975 and he is now an engineer in Nanjing Telecommunication Technology Institute, China. His research interests include RF tunable filters.